Finite Element Analysis on Double-Telescopic Prop of Hydraulic Support

WANG Xuewen*, YANG Zhaojian, liu hunju
College of Mechanical Engineering, Taiyuan University of Technology, Taiyuan 030024, PR China
*corresponding author, e-mail: wxuew@163.com

Abstract

According to Chinese coal industry standard MT313-1992 and European standard EN 1804-2-2001, using the modern CAE technology, based on the coupling meshing technology of structured grids and unstructured grids, the finite element strength analysis on 360-type double-telescopic prop is carried out under axial 1.5 times, axial 2.0 times rated load and off-center 0.3R 1.1 times rated load. The stability of the prop is studied using the buckling analysis. The results show that without regard to the dynamic load, the prop can bear 2.0 times axial pressure and 1.1 times off-center 0.3R pressure, and the stress distribution is even. Except the guide sleeve-I and the middle cylinder, other parts have high safety coefficient and can be optimized. The critical buckling load coefficient of the prop is 2.764, and the buckling instability of the type of prop will not happen if used under the rated working condition set by Chinese coal industry standard MT313-1992 and European standard EN 1804-2-2001. The paper can provide the basis for setting new related technology standard.

Keywords: Hydraulic support, Double-telescopic prop, Strength, Stability, Hybrid Grids

1. Introduction

In the past, it's always based on the experience or the test method to study the structure or the pressure of the hydraulic support and its props [1-3]. With the development of numerical simulation technology and finite element method [4] [5], it required that the double-telescopic prop's strength, stiffness and stability become higher and higher. Thus, it is required to clearly know the prop's stress response and mechanical properties. Using the modern CAE technology, based on the coupling meshing technology of structured grids and unstructured grids, this paper will do the finite element strength analysis on 360-type double-telescopic prop under axial 1.5 times, axial 2.0 times rated load and off-center 0.3R 1.1 times rated load, and the buckling analysis of the prop, according to Chinese coal industry standard MT313-1992—"The Technical Condition of Hydraulic Support Prop" [6] and European standard EN 1804-2-2001—"Machines for underground mines - Safety requirements for hydraulic powered roof supports - Part 2: Power set legs and rams" [7]. Based on the above analysis, the prop structural response to working loads will be studied in detail, and the design standards of MT313-1992 and EN 1804-2-2001 will be compare, to provide theoretical supports for the design of double-telescopic prop and setting new technology standards.

2. The Models

2.1 The Geometric Model

As shown in Figure 1, the double-telescopic prop mainly consists of the outer cylinder, the middle cylinder, the support pillar and two guide sleeves. The internal diameter of the outer cylinder is 360mm, the support pillar head diameter is 200mm, and the whole extending length of the prop is 4700mm.

To meet the structure shape, the geometric model is established using combining methods of Sweeping Representation [8] [9] and Constructive Solid Geometry (CSG) [10] [11] to carry out geometry and topology definition of the prop. The geometric model is as Figure1 shows, which properly revealed the spatial geometry relationship and the section shape of the prop.

2.2 The Finite Element Model

　　　　As shown in Figure 2, the geometric model is meshed using 3D solid element. In view of the complexity of the prop structure, the parts which have regular shape such as the cylinders are meshed by mainly low order element and structured grid which have the advantage of fast convergent rate in finite element analysis [12] [13], and the parts which have irregular shape such as the guide sleeves are meshed by mainly higher order element and unstructured grid [14] [15] which have the advantage of good adaptability. In addition, to make the finite element mesh to adapt to the boundary conditions, the meshing takes sudden geometry changes, load boundary, displacement boundary and so on into consideration. In short, the meshing process effectively balances the computing accuracy, computing scale and computing speed.
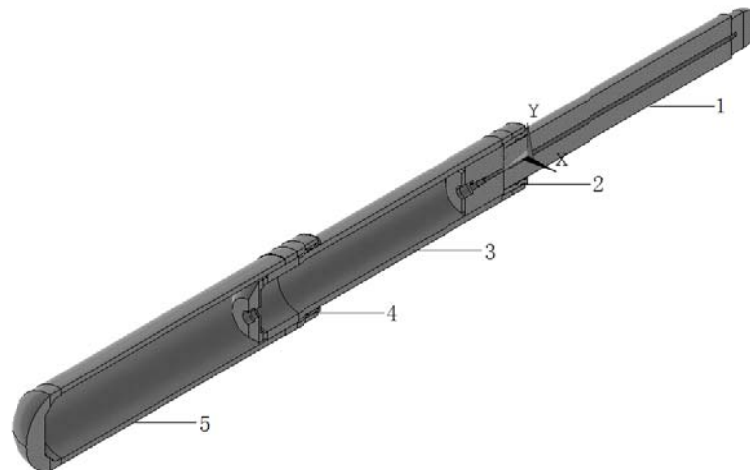
1-the support pillar; 2-the guide sleeve-I; 3-the middle cylinder;
4-the guide sleeve-II; 5- the outer cylinder

Figure 1. The geometric model (longitudinal section in center plane)

Figure 2. The finite element model

2.3 The Boundary Condition

　　　　The retraction stroke of the prop is S≤1300mm; The rated working resistance is F≤4500kN; In order to simulate the actual working condition, the contact models are established, and the contact elements are created in the connecting places between the support

pillar and the guide sleeve-I, the middle cylinder and the guide sleeve-I, the middle cylinder and the guide sleeve-II, and the outer cylinder and the guide sleeve-II; According to Chinese coal industry standard MT 313-1992, the strength analysis on the prop will be carried out under axial 1.5 times and off-center 30mm 1.1 times rated load;   According to European standard EN 1804-2-2001, the strength analysis on the prop will be carried out under axial 2.0 times and off-center 0.3R 1.1 times rated load (R=100mm); The buckling analysis will be carried out under the working condition of whole extending.

3. The Strength Analysis

The material of the prop is 27SiMn, and the material parameters of 27SiMn are as Table 1 show.

Table 1. The material parameters of 27SiMn

Material name	Young modulus	Poisson's ratio	Tensile strength	Yield limit
27SiMn	2.07×10^{11}Pa	0.3	980Mpa	835Mpa

3.1 Under Axial Load

According to Chinese coal industry standard MT 313-1992, while the prop rises to the whole extending, under 1.5 times axial rated load, the structural damage does not occur on the prop cylinders body and guide sleeves [6]; According to European standard EN 1804-2-2001, when the dynamic loads are ignored, the prop must be able to withstand a load of 2.0 times axial rated load [7].
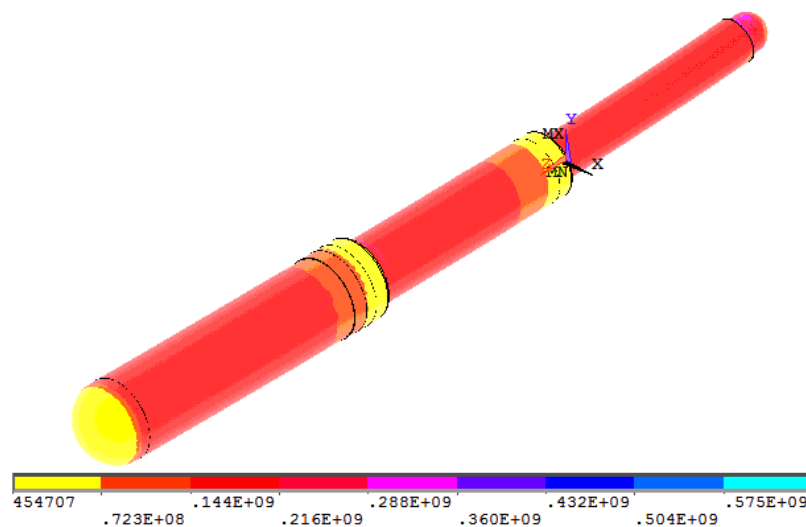
Figure 3. The stress distribution of the prop under 1.5 times axial rated load (Pa)

According to the above requirements, the strength analysis is carried out on the prop under 1.5 times and 2.0 times axial rated load. The calculating process is omitted, and the analysis results are as Figure 3, Figure 4, Figure 5, Figure 6 and Table 2 show.

In Figure 3 and Figure 4, MX is the Max VonMsie stress. The results show that the overall stress distribution of the prop is even, the Max stress under 1.5 times axial rated load is 575Mpa, and the Max stress under 2.0 times axial rated load is 767Mpa. The contact regions between the guide sleeve-I and the middle cylinder as well as a small part of the middle cylinder internal wall surface have larger stress concentration. Under 1.5 times axial rated load, the stress on these regions is about 450-510 Mpa, and under 2.0 times axial rated load, it is about 600~680 Mpa.
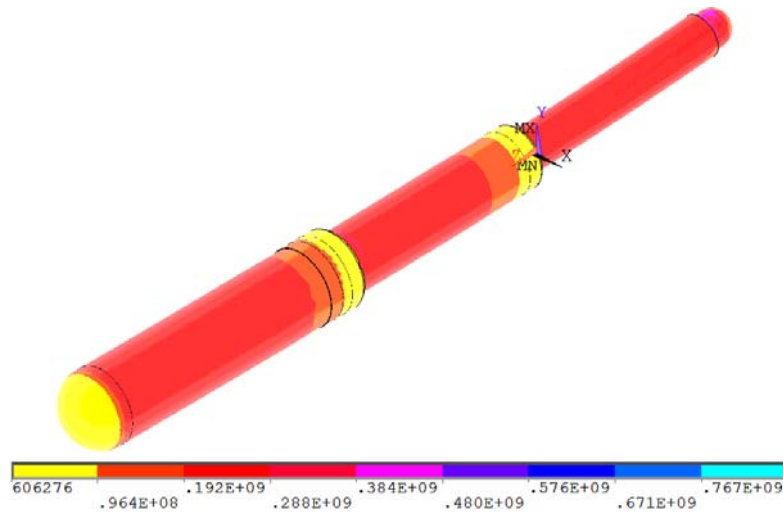
Figure 4. The stress distribution of the prop under 2.0 times axial rated load (Pa)
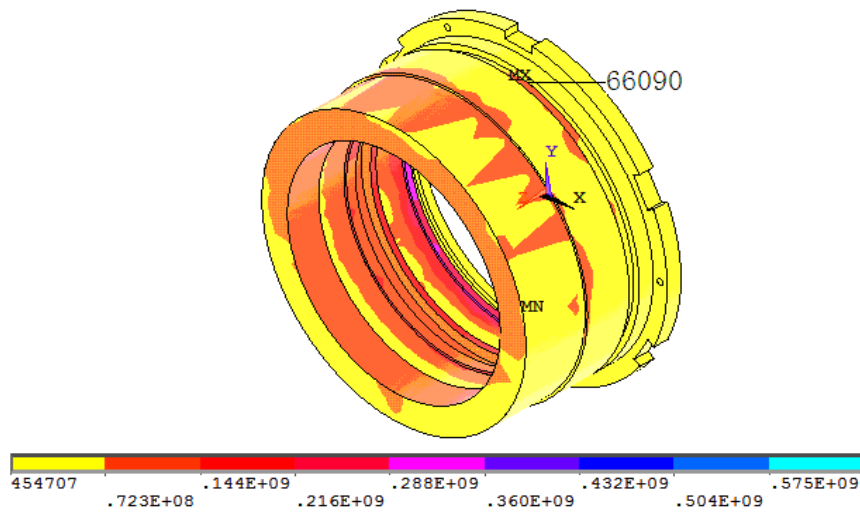
Figure 5. The stress distribution of the guide sleeve-I under 1.5 times axial rated load (Pa)
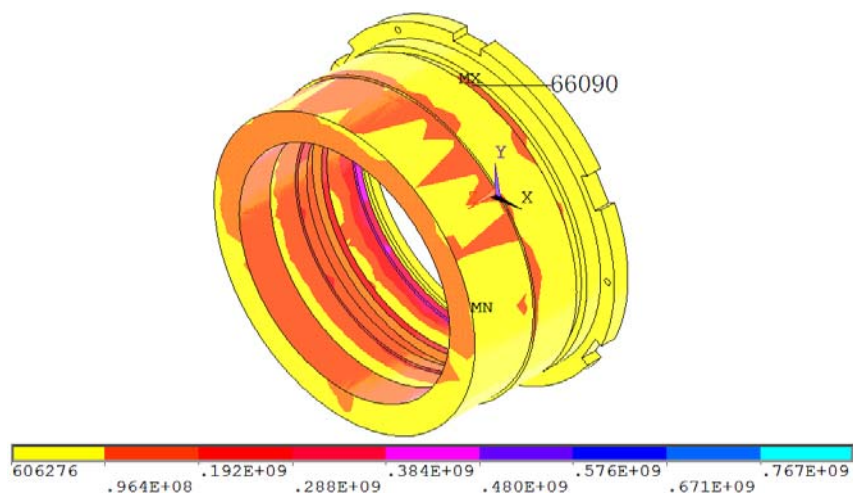
Figure 6. The stress distribution of the guide sleeve-I under 2.0 times axial rated load (Pa)

Table 2. The Max stress of the prop

Load	Axial		Off-center 30mm
	1.5 times	2.0 times	1.1 times
The node numbers	66090	66090	64690
The Max stress	575Mpa	767Mpa	681Mpa

No matter under 1.5 times or 2.0 times axial rated load, the node number of Max stress is №66090, which is within the guide sleeve-I (see Figure 5 and Figure 6). This is because when the prop rises to the whole extending, the contact between the guide sleeves and the cylinder body is non-rigid contact, thus the load transmitting is not fluent and causes local stress concentration. The results accords with the actual working condition of the prop.

By comparing Figure 3 with Figure 4, and Figure 5 with Figure 6, the structure stress changing is very similar under 1.5 times and 2.0 times axial rated load, which shows that the prop structure design is reasonable. The Max stresses are all smaller than material's tensile strength and yield limit, which meet the design requirements of Chinese coal industry standard MT313-1992 and European standard EN 1804-2-2001.

3.2 Under Off-center Load

According to Chinese coal industry standard MT 313-1992, while the prop rises to the whole extending, in the off-center 30mm place of the support pillar head, under 1.1 times rated load, the structural damage does not occur on the prop cylinders body and guide sleeves [6]; According to European standard EN 1804-2-2001, when doing the pressure misalignment test on the prop, the loading point is in the off-center 0.3R place of the support pillar head (R is the support pillar head radius), and the pier foundation diameter should be no more than 25% of the diameter of the outer cylinder, and the test pressure is 1.1 times ±5% of the rated load [7].
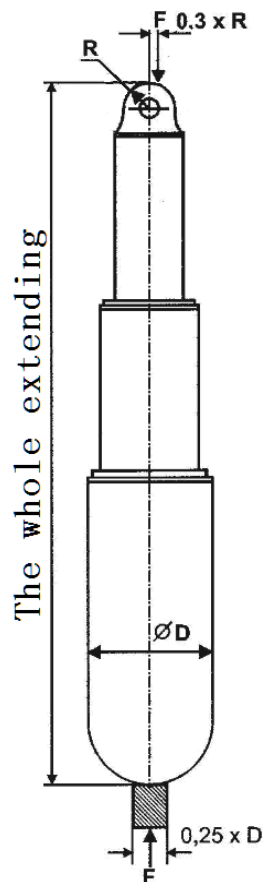
Figure 7. The boundary condition of strength analysis under off-center load

The support pillar head diameter of the 360-type double-telescopic prop is 200mm, that is, R=100mm, 0.3R=30mm. The standards of Chinese coal industry standard MT313-1992 and European standard EN 1804-2-2001 about this type of prop in the aspect of boundary condition of off-center distance are in accordance with each other. Thus, according to the provisions of both EN 1804-2-2001 and Chinese MT 313-1992, the boundary condition of strength analysis under off-center load of the 360-type double-telescopic prop is presented as Figure 7 shows. Where, R=100mm.

The calculating process is omitted, and the analysis results are as Figure 8, Figure 9 and Table 2 show.

In Figure 8 and Figure 9, MX is the Max VonMsie stress. The results show that the overall stress distribution of the prop is reasonable under the off-center 0.3R (30mm) 1.1 times rated load, but compared with the stress distribution under the axial load, the evenness is a little worse. The stress on one side with off-center load is bigger than that on the other side, especially on the outside wall of the support pillar and the internal wall of the two guide sleeves, in which the stress on one side with off-center load is obviously bigger than that on the other side, as shown in Figure 8 and Figure 9.
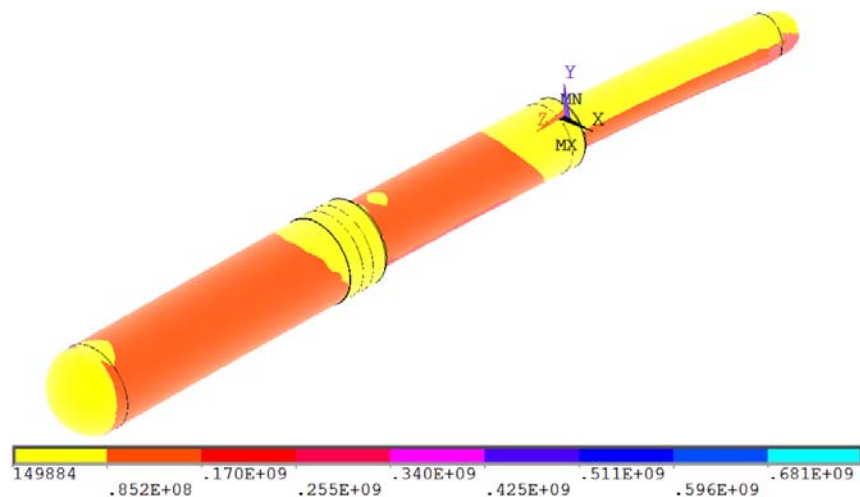
Figure 8. The stress distribution of the prop under 1.1 times off-center rated load (Pa)
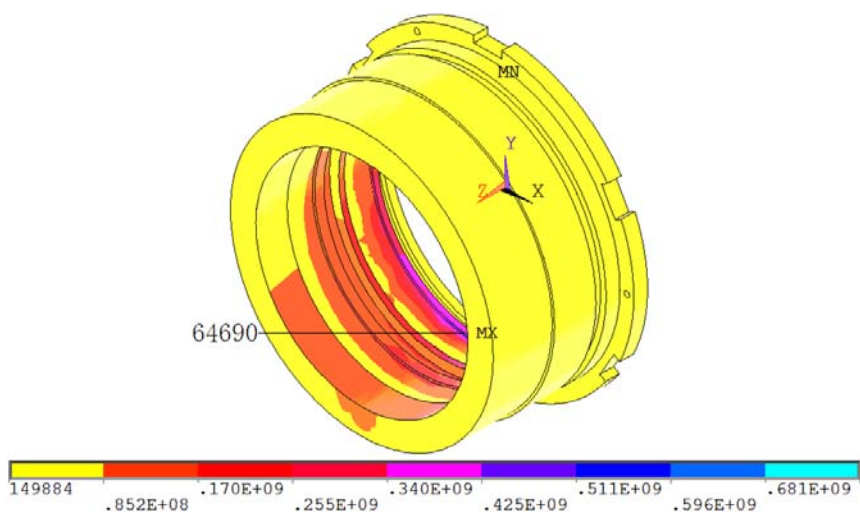
Figure 9. The stress distribution of the guide sleeve-I under 1.1 times off-center rated load (Pa)

The middle cylinder internal wall surface, the outer cylinder internal wall surface, and the contact regions between the guide sleeve-I and the middle cylinder have larger stress concentration. The stress on these regions is about 340-511 Mpa. The Max stress is 681Mpa, and the node number is №66090, which is within the guide sleeve-I (see Figure 9 and Table 2). This is because the off-center load leads to the prop bending, thus the prop bears the larger pressure stress on one side with off-center load, and because when the prop rises to the whole extending, the contact between the guide sleeves and the cylinder body is non-rigid contact, thus the load transmitting is not fluent and causes local stress concentration.

The results accord with the actual off-center load working condition of the prop, and the structure stress distributions meet the design requirements of Chinese coal industry standard MT313-1992 and European standard EN 1804-2-2001.

4. The Stability Analysis

When the transition from straight line balance state to curve balance state occurs on the prop, the prop will lose stability, which is called buckling. Compared with strength failure, the buckling shows completely different features. When the prop loses its stability, tiny outer disturbances will greatly cause structure deformation.
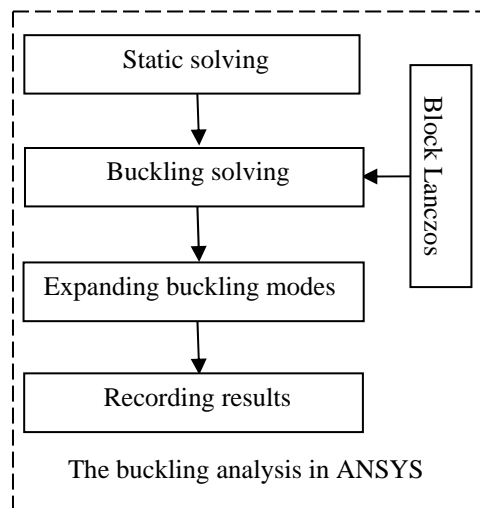
Figure 10. The buckling analysis process in ANSYS
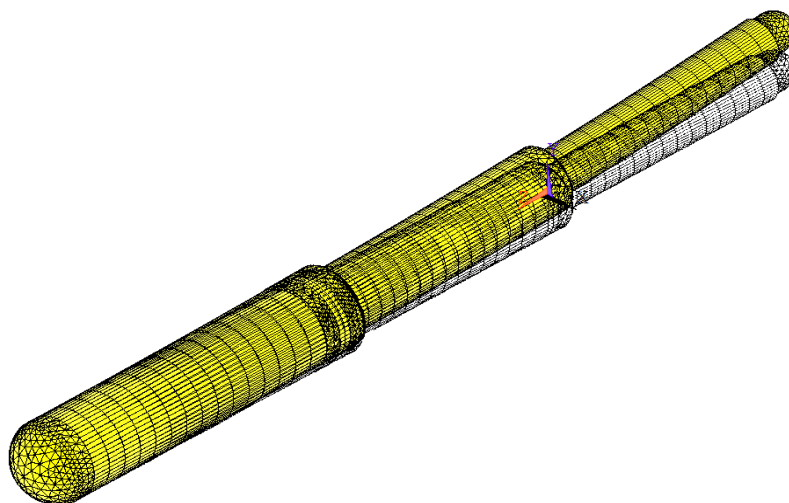
Figure 11. The buckling deformation

In general, the buckling analysis is a very complicated computational process for involving complicated elastic-plastic theory [16] [17]. The critical buckling load may be obtained by solving high order partial differential equation set. Usually only a few simple problems can be resolved accurately. In this paper, the finite element software ANSYS are used and the eigenvalue λ in equation (1) will be solve to study how much load will cause the lateral flexural-torsional buckling of the prop [18].

$$([K] + \lambda[S]) \{\psi\} = 0 \tag{1}$$

Where, [K] is stiffness matrix; λ is eigenvalue; [S] is stress stiffness matrix; {ψ} is displacement vector.

In equation (1), the displacement vector {ψ} is buckling shape, and the stress stiffness matrix [S] can strengthen or weaken the structure stiffness. In the calculation, by solving the eigenvalue λ, namely the scale factor of the stress stiffness matrix [S], which may bring the negative stiffness, the buckling load coefficient will be obtained. In ANSYS, the stiffness matrix [K] can play a role by activating the pre-stressed options.

In ANSYS [19], the buckling analysis results are buckling load coefficient. Multiply the buckling load coefficient by applied load to get the buckling load. If the applied unit load of 1N is given, the eigenvalue λ derived from equation (1) is the actual buckling load. It is obvious that the buckling load of this 360-type double-telescopic prop is sure to be bigger than the rated working pressure 4500kN, but in ANSYS, the allowed Max eigenvalue is 1000000, that is to say, under the applied unit load of 1N, the allowed Maximum buckling load is 1000kN, which is far smaller than 4500kN. To guarantee the correct convergence of buckling analysis, 10kN is given as the applied unit load.

The calculating process is as the Figure 10 shows using Block Lanczos method to get buckling mode. Through calculation, the eigenvalue is 1243.6, and the buckling distortion is as the Figure 11 shows.

The applied load is 10kN, and the eigenvalue is 1243.6. It means that when this prop is fully extended, the buckling load is 10kN×1243.6=12436kN, which is to say, when the load reaches 12436kN, the prop loses its loading capacity. 12436kN/4500kN=2.764 means that the buckling safety coefficient of the prop is 2.746.

5. Conclusion

1) The strength analysis results show that the structural strength of the 360-type double-telescopic prop meet the design requirements of Chinese coal industry standard MT313-1992 and European standard EN 1804-2-2001. When fully extended, the prop can bear 2.0 times axial pressure and 1.1 times off-center 0.3R load, and the overall stress distribution of the prop is even and the load transmitting is reasonable. Furthermore, because the contact between the guide sleeves and the cylinder body is non-rigid contact, the load transmitting is not fluent and causes local stress concentration, but the stress results meet the design requirements. Except the guide sleeve-I and the middle cylinder, other parts have high safety coefficient and can be optimized.

2) The buckling analysis results show that used under the rated working condition set by Chinese coal industry standard MT313-1992 and European standard EN 1804-2-2001, the lateral flexural-torsional buckling will not occur in the 360-type double-telescopic prop.

3) By comparing with European standard EN 1804-2-2001, Chinese coal industry standard MT313-1992 has lower design requirements on mechanical performance of hydraulic support prop. With the increasing of the mining height and the working resistance, and with the improvement of the demanding in strength, stability, safety and reliability of hydraulic support prop, the design conditions of Chinese coal industry standard MT313-1992 can be considered to improve.

References

[1] C González-Nicieza, A Menéndez-Díaz, AE Álvarez-Vigil, MI Álvarez-Fernández. Analysis of support by hydraulic props in a longwall working. *International Journal of Coal Geology*. 2008; 74(1): 67-92.
[2] Cao LM, Zeng QL Xiao XY. *Accounting Method of Intensity for Double Telescopie Props of Hydraulic Supports*. 2011 International Conference on Industry, Information System and Material Engineering. Guangzhou. 2011; 204-210: 1231-1234.
[3] R Juárez-Ferreras, C González-Nicieza, A Menéndez-Díaz, AE Álvarez-Vigil, MI Álvarez-Fernández. Measurement and analysis of the roof pressure on hydraulic props in longwall. *International Journal of Coal Geology*. 2008; 75(1): 49-62.
[4] Sekhara Rao, EVC Prasad, PVN. Finite element method using PDETOOL of matlab for hybrid stepper motor design. *Telkomnika*. 2012; 10(4): 680-686.
[5] Yongjuan Zhao, Yutian Pan, Meixia Huang. Numerical simulation of chip formation in metal cutting process. *Telkomnika*. 2012; 10(3): 486-492.
[6] Chinese coal industry standard. MT 313-1992. *The Technical Condition of Hydraulic Support Prop*. Beijing: China coal industry press; 1992.
[7] EN safety requirement standards. EN 1804-2-2001. *Machines for underground mines - Safety requirements for hydraulic powered roof supports - Part 2: Power set legs and rams*. EN safety press; 2001.
[8] Hüseyin Erdim, Horea T. Ilieş. Classifying points for sweeping solids. *Computer-Aided Design*. 2008; 40(9): 987-998.
[9] Frank Y Shih, Vijayalakshmi Gaddipati. Geometric modeling and representation based on sweep mathematical morphology. *Information Sciences*. 2005; 171(1-3): 213-231.
[10] Yang, Xue, Satvat, Nader. MOCUM: A two-dimensional method of characteristics code based on constructive solid geometry and unstructured meshing for general geometries. *Annals of Nuclear Energy*. 2012; 46: 20-28.
[11] Edwin Boender, Willem F. Bronsvoort, Frits H. Post. Finite-element mesh generation from constructive-solid-geometry models. *Computer-Aided Design*. 1994; 26(5): 379-392
[12] PA Durbin, G Iaccarino. An Approach to Local Refinement of Structured Grids. *Journal of Computational Physics*. 2002; 181(2): 639-653.
[13] Zhu ZQ, Wang P, Tuo SF, Liu ZA. Structured/unstructured grid generation method and its application. *Acta Mechanica*. 2004; 167(3-4): 197-211.
[14] ZHANG M. Modeling of radiative heat transfer and diffusion processes using unstructured grid. USA: Tennessee Technological University; 2000.
[15] CC Su, KC Tseng, JS Wu, HM Cave, MC Jermy, YY Lian. Two-level virtual mesh refinement algorithm in a parallelized DSMC Code using unstructured grids. *Computers & Fluids*. 2011; 48(1): 113-124.
[16] HA El-Ghazaly, AN Sherbourne. Deformation theory for elastic-plastic buckling analysis of plates under nonproportional planar loading. *Computers & Structures*. 1986; 22(2): 131-149
[17] Miquel Casafont, Frederic Marimon, Magdalena Pastor, Miquel Ferrer. Linear buckling analysis of thin-walled members combining the Generalised Beam Theory and the Finite Element Method. *Computers & Structures*. 2011; 89(21–22): 1982-2000
[18] José Luis Manzanares Japón, Ignacio Hinojosa Sánchez-Barbudo. Non-linear plastic analysis of steel arches under lateral buckling. *Journal of Constructional Steel Research*. 2011; 67(12): 1850-1863
[19] A Ghorbanpour Arani, R Rahmani, A Arefmanesh. Elastic buckling analysis of single-walled carbon nanotube under combined loading by using the ANSYS software. *Physica E: Low-dimensional Systems and Nanostructures*. 2008; 40(7): 2390-2395